Article ID: 1006-8775(2020) 01-0001-13

OPERATIONAL FORECAST OF RAINFALL INDUCED BY LANDFALLING TROPICAL CYCLONES ALONG GUANGDONG COAST

LI Qing-lan (李晴岚) [1], LIU Bing-rong (刘炳荣) [1], WAN Qi-lin (万齐林) [2], WANG Yu-qing (王玉清) [3], LI Guang-xin (李广鑫) [1], LI Tie-jian (李铁键) [4] , LAN Hong-ping (兰红平) [5], FENG Sheng-zhong (冯圣中) [1], LIU Chun-xia (刘春霞) [2]

(1. Shenzhen Institute of Advanced Technology, Chinese Academy of Sciences, Shenzhen, Guangdong 518055 China; 2. Guangzhou Institute of Tropical and Marine Meteorology, CMA, Guangzhou 510641 China; 3. University of Hawaii at Manoa, Honolulu, HI 96822 USA; 4. Department of Hydraulic Engineering, Tsinghua University, Beijing 100084 China; 5. Shenzhen Meteorological Bureau, Shenzhen, Guangdong 518040 China)

Abstract: Following previous studies of the rainfall forecast in Shenzhen owing to landfalling tropical cyclones (TCs), a nonparametric statistical scheme based on the classification of the landfalling TCs is applied to analyze and forecast the rainfall induced by landfalling TCs in the coastal area of Guangdong province, China. All the TCs landfalling with the distance less than 700 kilometers to the 8 coastal stations in Guangdong province during 1950—2013 are categorized according to their landfalling position and intensity. The daily rainfall records of all the 8 meteorological stations are obtained and analyzed. The maximum daily rainfall and the maximum 3 days' accumulated rainfall at the 8 coastal stations induced by each category of TCs during the TC landfall period (a couple of days before and after TC landfalling time) from 1950 to 2013 are computed by the percentile estimation and illustrated by boxplots. These boxplots can be used to estimate the rainfall induced by landfalling TC of the same category in the future. The statistical boxplot scheme is further coupled with the model outputs from the European Centre for Medium-Range Weather Forecasts (ECMWF) to predict the rainfall induced by landfalling TCs along the coastal area. The TCs landfalling in south China from 2014 to 2017 and the corresponding rainfall at the 8 stations area are used to evaluate the performance of these boxplots and coupled boxplots schemes. Results show that the statistical boxplots scheme and coupled boxplots scheme can perform better than ECMWF model in the operational rainfall forecast along the coastal area in south China.

Key words: tropical cyclone; coastal area; rainfall forecast; statistical boxplot scheme; coupled boxplot scheme

CLC number: P444 **Document code:** A

https://doi.org/10.16555/j.1006-8775.2020.001

1 INTRODUCTION

Tropical cyclone (TC) is one of the most lethal and powerful natural phenomena, especially in China (Ren et al. [1]; Xiao et al. [2]). TCs will usually bring heavy rainstorm in the coastal area, which may cause catastrophic flood and mudslide, resulting in tremendous loss of lives and property (Rappaport et al. [3]; Li et al. [4]). Timely warning of the possible disasters caused by TCs is therefore essential for the local authority to protect people, which demands accurate and timely forecast of rainfall induced by TCs.

Received 2019-04-28; **Revised** 2019-12-15; **Accepted** 2020-02-15

Foundation items: Key Research and Development Projects in Guangdong Province (2019B111101002); Program of Science, Technology and Innovation Commission of Shenzhen Municipality (JCYJ20170413164957461, GGFW2017073114031767)

Biography: LI Qing-lan, Ph. D., primarily undertaking research on quantitatively forecast of wind and rainfall induced by landfalling and offshore tropical cyclones, and tropical cyclones' intensity forecast.

Corresponding author: LI Qing-lan, e-mail: ql.li@siat.ac.cn

Although there are urgent demands, the prediction of local rainfall induced by TCs is very hard and challenging (Businger et al. [5]; AMS [6]; Willoughby et al. [7]). Nowadays, Numerical Weather Prediction (NWP) models perform well in forecasting the track of TCs, but the forecast of TC rainfall by NWP models remains problematic (Willoughby et al. [7]; Roy and Kovordanyi [8]). NWP is still not good enough to capture the complicated intrinsic dynamic processes of TCs and the environmental conditions, which are strongly related to the precipitation induced by TCs (Saha et al. [9]). It is reported that the rainfall is related to the geographical location and the intensity of TC (Lonfat et al. [10]). Precipitation decreases logarithmically with the distance from the center of TC (Riehl and Malkus [11]; Simpson and Riehe [12]; Kidder et al. [13]). Besides, the precipitation and the intensity of TC have a significantly positive correlation (Pfost [14]). Furthermore, the distribution of the precipitation induced by TCs is not symmetric and the rainfall usually concentrates on one side of the track of a TC (Elsberry [15]; Corbosiero and Molinari [16]). In the Northern Hemisphere, landfalling TC will usually induce stronger rainfall on the right hand side than on the left hand side, as different surface friction between land and water may lead to low level

convergence and bring more moisture to the right hand side when a TC approaches the coast (Kimball [17]; Li et al. [18]). Researchers pay much attention to pursue a more reliable approach than NWP to forecast the rainfall induced by TCs. Mark et al. [19] proposed a Rainfall Climatology and Persistence model (R-CLIPER) which gave a description of the spatial and temporal distribution of rainfall induced by a TC. The rainfall climatology was described as a relationship with the radius and time after landfall. However, the model resulted in a circularly symmetric rainfall distribution, which was not true in reality. By incorporating the impact of vertical shear and topography into the original R-CLIPER, Lonfat et al. [20] developed the Parametric Hurricane Rainfall Model (PHRaM). PHRaM made some improvement in the prediction in terms of the rainfall spatial distribution and amplitude compared with R-CLIPER. However, the model showed a significant bias toward lower rain amount when the rainfall prediction at a distance far away from the storm center, such as 300-400km. Phost [14] identified the moving speed of a TC as the key factor for estimating the maximum landfalling-TC-induced rainfall along the northern Gulf of Mexico coast and Florida peninsula. However, there was no method proposed in the study to forecast the rainfall along the TC swath except for the maximum rainfall.

Guangdong province, located in south China with 4114 kilometers of coastline, is one of the most vulnerable areas to TC disasters in China. The province suffers great loss from landfalling TCs every year (Liang et al. [21]; Ye [22]; Yuan et al. [23]). In fact, even a slight typhoon may lead to severe economic loss in this region (Yin et al. [24]). Typhoon Mujigae in 2015 hit Guangdong province in October, bringing powerful winds and heavy rainfall as it approached the province. It affected more than 3.5 million people and devastated over 3000 houses and 282 thousand hectares of cropland (Xinhuanet News [25]). To protect people from such kind of natural disaster, decision-makers need to issue timely and accurate TC warnings. However, in China, there are few operational quantitative precipitation forecast techniques and the prediction of local rainfall induced by TC mainly relies on the empirical estimation and subjective experience of forecasters with the help of NWP models (Chen et al. [26]; Xu et al. [27]). Therefore, it is necessary to develop and improve the quantitative precipitation forecast techniques based on the knowledge of rainfall induced by TCs in this area. Li et al. [18] developed an operational statistical scheme to forecast rainfall induced by TCs in Shenzhen and it performed well. In this study, the scheme proposed by Li et al. [18] will be further improved to couple with NWP to forecast the precipitation due to TCs at several coastal meteorological stations in Guangdong province. The performance of the improved scheme in the study area will be evaluated.

This paper consists of four parts. Section 2 will introduce the data and methodology. Section 3 will detail the procedures, results and discussions. The summary and conclusion will be presented in section 4.

2 DATA AND METHODOLOGY

2.1 *Data*

Eight coastal stations are involved in this study; namely, they are stations of Nanao, Shanwei, Shenzhen, Zhuhai, Shangchuan Island, Yangjiang, Zhanjiang, and Xuwen, respectively (from east to west). The information of these stations is listed in Table 1.

Table 1. The details of the 8 coastal stations.

Stations	Abbreviation	Duration of rainfall data
Nanao	NA	1957-2017
Shanwei	SW	1952-2017
Shenzhen	SZ	1952-2017
Zhuhai	ZH	1961-2017
Shangchuan Island	SCI	1957-2017
Yangjiang	YJ	1952-2017
Zhanjiang	ZJ	1951-2017
Xuwen	XW	1956-2017

The daily rainfall records of these eight stations are obtained from China Meteorological Administration (CMA), which starts from 8pm (Beijing time) of the previous day to 8pm of the current day. From 1951-2017, there are 674 TCs landfalling in south China. The TC characteristics, including TC landfalling intensity, landfalling time and position, are obtained from CMA as well. Historical TC and rainfall data before December 31, 2013 are used for the calibration of the forecasting scheme in this study and the data after 2013 are used for the validation of the scheme.

2.2 *Methodology*

2.2.1 TC CLASSIFICATION

Following the method of Li et al.[18], the landfalling TCs are divided into group A and group B for each of the coastal stations. Different from Li et al.[18], we employed a grouping method based on the different wind direction at the station, i.e., the onshore wind or the offshore wind, rather than the landing direction of east or west. Group A contains the TCs which bring onshore wind to those stations. For Nanao (NA), Shanwei (SW), Shenzhen (SZ), Zhuhai (ZH), Shangchuandao Island (SCI) and Yangjiang (YJ), the corresponding TCs of group A are those TCs landing to the west of the specific station; however, for the station of Zhanjiang (ZJ) and Xuwen (XW), the corresponding TCs of group A are those landing to the south of the specific station. In contrast, group B contains TCs landing on the other side which brings offshore wind to the corresponding stations. Also based on Li et al.[18], all the TCs landfalling within the distance of 700 kilometers to each

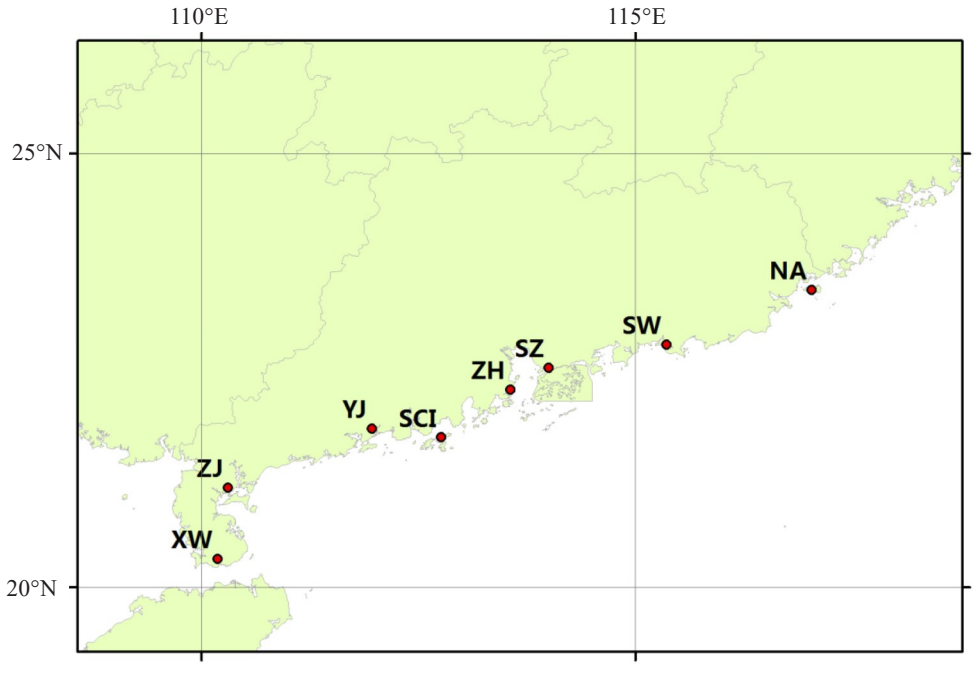

Figure 1. Locations of the 8 coastal stations.

of the specific station are considered. According to the distance between the TC landfalling position and the specific station, TCs are further grouped into A1, A2, A3, … , A7, B1, B2, …, B7, based on the criteria of 100 kilometers and wind directions. For each station, A1 group refers to TCs with the distance of 0-100 km (including 100 km) to the station, bringing onshore wind to the corresponding station; A2 group contains TCs with the distance of 101-200 km to the station, bringing onshore wind to the corresponding station, etc. Group B7 then contains TCs with the distance of 601-700 km to the station, bringing offshore wind to the corresponding station.

According to the TC intensity criterion of China Meteorological Administration which is shown in Table 2, there are six categories of TCs, i. e. super typhoon (SuperTY), severe typhoon (STY), typhoon (TY), severe tropical storm (STS), tropical storm (TS) and tropical depression (TD) based on the maximum wind speed near the TC center. In accordance with Li et al.[18], all these TCs are grouped into four categories in this study, i. e., TTY(including SuperTY, STY, and TY), STS, TS and TD. Thus, according to their landfalling direction, landfalling distance and landfalling intensity, all the TCs are classified into A1-TTY, A1-STS, A1-TS, A1-TD, A2-TTY, A2-STS, A2-TS, A2-TD, … , B7-TTY, B7-STS, B7-TS, and B7-TD. Finally, all the landfalling TCs are classified into 56 groups.

Table 2. Categories of TC based on the intensity criterion of China Meteorological Administration.

Category	Abbreviation	Sustained maximum wind speed near center
Super Typhoon	SuperTY	>=51m s^{-1}
Severe Typhoon	STY	41.5 m s^{-1} ~ 50.9 m s^{-1}
Typhoon	TY	32.7 m s^{-1} ~ 41.4 m s^{-1}
Severe Tropical Storm	STS	24.5 m s^{-1} ~ 32.6 m s^{-1}
Tropical Storm	TS	17.2 m s^{-1} ~ 24.4 m s^{-1}
Tropical Depression	TD	10.8 m s^{-1} ~ 17.1 m s^{-1}

2.2.2 RAINFALL DATA PROCESSING

In the late 1980s, China Meteorological Administration began to record hourly weather variables. Before the 1980s, rainfall was recorded on a daily basis. In order to have sufficient rainfall record, the influence of rainfall induced by landfalling TCs is computed on a daily basis in this study. The maximum daily rainfall caused by TCs is the maximum value of the rainfall records during the landfalling period, which is defined as the period from two days before TC landfall to three days after landfall[18]. As the landing time for a TC might vary from 00 to 23 in a day, only computing the maximum daily rainfall is not enough to reflect the influence due to a landfalling TC. Therefore,

the maximum 3-day accumulative rainfall is computed as well, which is the maximum three consecutive days accumulative rainfall during the landfalling period.

2.2.3 BOXPLOT

Due to the daily rainfall's non-normal distribution characteristics, non-parametric statistical methods are more appropriate for analyzing the rainfall data (Pett[28]; Wilks[29]; Li et al.[18]). Boxplot is an efficient and widely used graphic tool for data analysis (Tukey[30]). There are six elements in a boxplot, including the median, the lower quartile, the upper quartile, the lower whisker, the upper whisker and the outliers, all of which can be calculated from the samples.

In this study, after the landfalling TCs are categorized for each station, the corresponding rainfall records at the station due to each TC group can be analyzed by boxplot method. In practical application, according to the track and intensity forecast by NWP models and the experience of forecasters, the category of the TC, i.e. TTY, STS, TS, TD, can be determined 12-36 hours in advance if the TC is going to land along the coast of south China. Then, referring to the boxplot of the specific TC group that the landfalling TC belongs to, forecasters can obtain an estimation of the maximum daily rainfall and the maximum 3-day accumulated rainfall that the landfalling TC may cause, including the medians, the interquartile ranges, etc.

2.2.4 COUPLING ECMWF NWP OUTPUT WITH THE HISTORICAL RECORDS

Rainfall is a stochastic process in time and in space (Johnson et al.[31]; Chowdhury et al.[32]; Onyutha and Willems[33]). Although the distribution for a particular rainfall event is stochastic, the rainfall amount at a station for long time is stable and will have similar pattern with its nearby area. Therefore, the boxplot of the historical rainfall induced by a TC group which reflects the stochastic rainfall characteristics in time at the corresponding station can approximately be treated as the spatial rainfall distribution pattern for the nearby area at a rainfall event.

Meanwhile, NWP model can roughly reflect the atmospheric condition of a TC process although the model is not good enough to capture the complicated intrinsic dynamic processes of the TCs. Therefore, the rainfall prediction provided by the NWP model can be also used as an important reference for forecasters. European Centre for Medium-Range Weather Forecasts (ECMWF) model is renowned worldwide for providing the most accurate medium-range global weather forecast (Halperin et al.[34]; Wang et al.[35]; Magnusson et al.[36]). This study will couple the weather forecast information from ECMWF model with the historical observation data to generate a more accurate forecast for TC rainfall at the coastal area. Generally, ECMWF model tends to underestimate the amount of rainfall induced by heavy storm; however, it performs well in forecasting light rainfall (Zhong et al.[37]). For each TC, the rainfall forecast for the corresponding station (EC_{st}) and rainfall extreme forecast, including the maximum of the predicted rainfall (EC_{max}) and the minimum of the predicted rainfall (EC_{min}), for the city area (the city which contains the station) by ECMWF model can be used as references to adjust the rainfall forecast by the boxplot scheme. Three ways are proposed to adjust the boxplot scheme, which are described in detail as follows.

The 50% quantile scheme

The key step for this scheme is to adjust the upper bound and the lower bound according to the EC_{st}. While the EC_{st} is greater than the 75% percentile of the boxplot, the upper bound is the bigger one of the EC_{max} and the maximum of the boxplot. And the lower bound is the median of the boxplot. While the EC_{st} is less than the 25% percentile of the boxplot, the lower bound is the smaller one of the EC_{min} and the minimum of the boxplot. And the upper bound is the median of the boxplot. Otherwise, the upper bound is the 75% percentile of the boxplot and the lower bound is 25% percentile of the boxplot.

The 100% quantile with ECMWF model extreme minimum scheme

The upper bound is the maximum of the boxplot and the lower bound is the smaller one of the EC_{min} and the minimum of the boxplot. Through this adjustment, the scheme will include more information of the unbalanced rainfall distribution which is neglected by the boxplot method, although the lower bound of the rainfall is not the key point of typhoon rainfall forecast.

The full quantile scheme with ECMWF model extreme outputs

In this scheme, the upper bound is the bigger one of the EC_{max} and the maximum of the boxplot. The lower bound is the smaller one of the EC_{min} and the minimum of the boxplot. This scheme can reflect the potential maximum area's rainfall range for the coming precipitation due to a TC.

2.2.5 THE ESTIMATION OF ACCURACY

In order to evaluate the performance of the coupled statistical boxplot scheme and the ECMWF model in forecasting TC induced rainfall, quantitative estimation of the accuracy is conducted. In each specific city which contains a coastal national basic meteorological station, there are numbers of other automatic weather stations recording rainfall. For each rainfall event, it is not easy to predict well the exact rainfall at a specific station. However, people and the local authorities will usually care about the potential maximum rainfall in a certain area. ECMWF model can provide a rainfall range for the whole urban area, while the coupled statistical boxplot scheme can also provide a rainfall range. Suppose there are altogether a stations in the city and there are x stations with the rainfall record between the upper bound and the lower bound of the forecast, the accuracy of the forecasting would then be $\frac{x}{a}$ (Yates et al.[38]).

3 RESULTS AND DISCUSSIONS

3.1 *Boxplots for the precipitation*

All the TCs landfalling within the distance of 700 kilometers to the eight meteorological stations are taken into account. Following the procedures mentioned in section 2, the historical landfalling TCs from 1950 to 2013 are grouped into 56 categories. For all the historical rainfall records, the non-parametric statistical method is employed in the analysis. The maximum daily rainfall (R24) and the 3-day accumulated rainfall (R72) during the TC landfalling period for each TC category at each station are estimated and the results are described by the statistical boxplot scheme.

Figure 2 shows the boxplots of R24 (Fig. 2a) and R72 (Fig. 2b) for each TC category during the TCs landfalling period at Shenzhen and Zhuhai, for instance. In each figure, the subgraphs from the top to the bottom illustrate the rainfall characteristic of the groups which belong to TTY, STS, TS, and TD, respectively. In each subgraph, the thick black solid line in the middle represents the position of the meteorological station, while the ticks of the horizontal coordinate-axis indicate the distance to the station. For example, A1 represents the TCs landfalling within the distance of 100 km which bring onshore wind to the stations; B1 represents the TCs landfalling within the distance of 100 km which bring offshore wind to the station. From Fig. 2, it can be seen that the maximum daily rainfall and 3-day accumulated rainfall induced by different types of TCs at Shenzhen and Zhuhai have similar patterns. In general, with the increase of distance, the rainfall induced by landfalling TCs tends to be weaker and the decreasing rate of this tendency becomes slower. With the same landfalling distance and direction, TTY will generally bring more rainfall to the stations than STS and TS do, especially within the distance of 300 km to the stations. The boxplots of the precipitation due to TCs landfalling on the left side and the right side are not symmetric along the central thick black solid line, especially for the TD category. Compared with the TCs landfalling on the right side which bring offshore wind to the corresponding station, TCs landfalling on the left side which bring on shore wind to the station may generally induce stronger rainfall.

It is worth mentioning that the weather observation in Zhuhai starts from September 1961, which is later than the observation in Shenzhen. Zhuhai station is located to the west of Shenzhen station with a distance of around 70 kilometers. For this reason, most of the TCs in group B1 at Zhuhai station will be categorized into group A1 at Shenzhen station. Similarly, most TCs in group A1 at Zhuhai station will be categorized into group A2 at Shenzhen station.

3.2 *Cases evaluation: forecasting and discussion*

During the year from 2014 to 2017, there are altogether 25 TCs landfalling in the north of Vietnam and along the coastline of south China. The detailed information of these landfalling TCs is listed in Table 3. These TCs are used to evaluate the performance of the coupled statistical boxplot scheme.

For a specific station, according to the landfalling position and intensity, the TCs in table 3 will be classified individually. Then the TC-induced rainfall at a city area can be figured out according to the boxplot scheme. Meanwhile, the rainfall forecast by ECMWF model can also provide a rainfall range for the city area, including the EC_{st}, EC_{min} and EC_{max}. With the reference of ECMWF models outputs, the lower bound and the upper bound of rainfall forecast for each of the coupled statistical boxplot scheme can be computed as well, according to the methods mentioned in section 2.2.4.

By comparing the forecast accuracy of the rainfall forecast by ECMWF model and by the coupled statistical boxplot schemes, we can estimate the performance of each scheme. The average forecasting accuracy for each of the forecasting schemes is presented in Table 4 and Table 5. Furthermore, the forecasting accuracy at the national basic stations by each of the forecasting schemes is computed, and the results are presented in Table 4 and Table 5 as well.

Compared with the rainfall forecast at the AWSs over the city area by ECMWF model, the forecasts by the coupled statistical schemes are generally better. The 50% quantile scheme and the 100% quantile scheme without extreme ECMWF output perform better and have higher accuracy at 7 cities compared with the forecast by ECMWF model except for ZJ city. The full quantile scheme with the extreme output of ECMWF and the 100% quantile scheme with EC_{min}, which consider the advantages of ECMWF model and statistical scheme, overwhelm the ECMWF model's forecast at all the 8 cities. As the statistical boxplot scheme mainly considers the maximum daily rainfall or maximum 3-day accumulative rainfall, the high rainfall range over the area might be covered by the scheme. For the coupled scheme including the EC_{min}, as well as the scheme including ECMWF extreme output (including EC_{max} and EC_{min}), the rainfall range certainly becomes larger, especially enlarging the lower rainfall range, which will therefore improve the forecast accuracy over the city area. Furthermore from Table 4 and Table 5, it can be seen that the forecasting accuracy at the national basic stations is generally higher than the forecasting accuracy at the AWSs by the forecasting schemes. This is reasonable as those forecasting schemes are originally developed based on the historical rainfall observations of the national basic station.

From Table 4 and Table 5, it can be seen that the coupled statistical schemes perform well in forecasting the rainfall induced by TCs along the coastal area in Guangdong province. It should be pointed out that though the extreme minimum of ECMWF model improves the forecast accuracy of the statistical scheme,

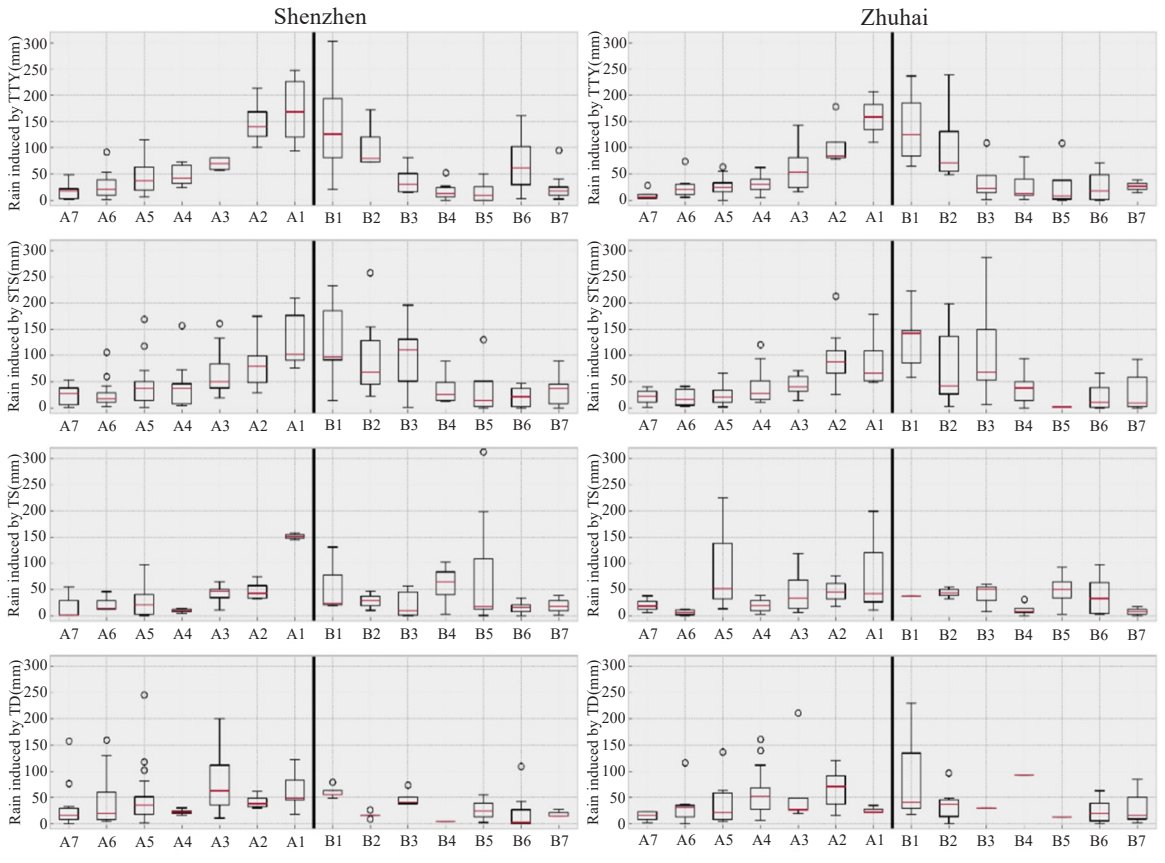

(a)

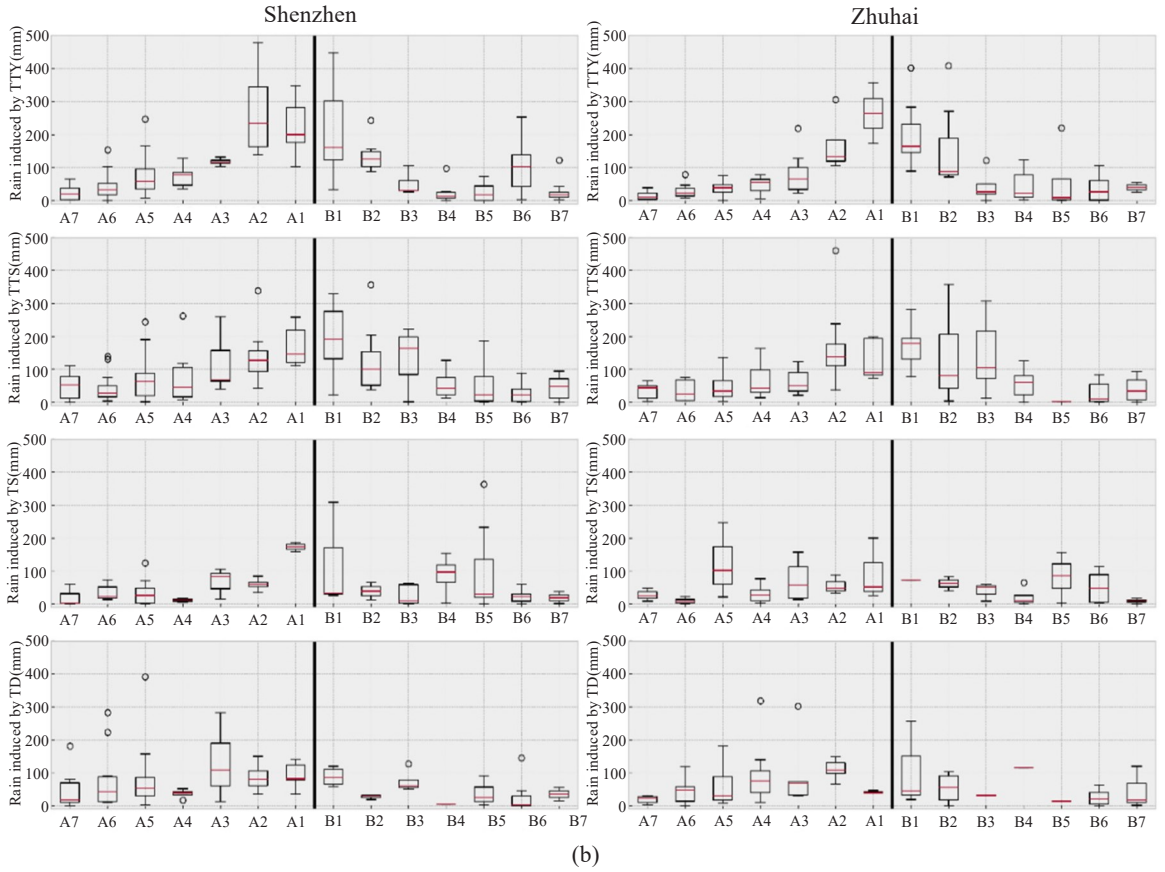

(b)

Figure 2. Boxplots of the maximum daily rainfall (a) and 3 days accumulated rainfall (b) induced by different TC categories during landfalling period in Shenzhen from 1952 to 2013 (left) and in Zhuhai from 1961 to 2013 (right): the first row is for TTY, the second row is for TTS, the third row is for TS and the fourth row is for TD.

Table 3. The details of the 25 TCs landfalling within the distance of 700 km to the 8 coastal stations in Guangdong province during the period from 2014 to 2017.

Name	Year	Landing longitude (°E)	Landing latitude (°N)	Landing intensity (m s^{-1})
HAGIBIS	2014	116.7	23.2	20
RAMMASUN	2014	110.3	20.3	55
KALMAEGI	2014	110.9	19.8	40
MATMO	2014	119.5	25.2	33
2014TD	2014	110.4	21.1	12
KUJIRA	2015	110.5	18.9	25
LINFA	2015	116.2	22.8	35
SOUDELOR	2015	119.2	25.1	38
DUJUAN	2015	119.1	25.1	33
MUJIGAE	2015	110.6	21.1	50
NEPARTAK	2016	118.7	24.7	25
MIRINAE	2016	110.2	18.7	28
NIDA	2016	114.5	22.5	40
DIANMU	2016	110.5	20.6	20
MERANTI	2016	118.3	24.5	50
MEGI	2016	118.9	25	33
SARIKA	2016	110.4	18.8	45
HAIMA	2016	115.1	22.8	42
2016TD	2016	112.5	21.8	14
MERBOK	2017	114.5	22.5	23
ROKE	2017	114.3	22.4	20
HAITANG	2017	119.5	22.5	20
NESAT	2017	119.5	25.5	33
HATO	2017	112.9	22	42
PAKHAR	2017	112.9	22	30

Table 4. Comparisons of the average accuracy of daily rainfall forecast induced by TCs at the 8 cities by ECMWF model (the second and third column), by the pure boxplot method (the last two columns) and by the coupled statistical schemes (the fourth to the ninth column) from 2014 to 2017. The numbers with normal font style in the table refer to the average accuracy of the rainfall forecast at the AWSs for the corresponding city, and the italic bold numbers refer to the average accuracy of the rainfall forecast at the national basic stations of the corresponding cities.

City	The accuracy of EC		The 50% quantile scheme		The 100% quantile scheme with EC_{min}		The full quantile scheme with ECMWF extreme outputs		The 100% quantile scheme without ECMWF extreme output	
NA	0.02	***0.06***	0.40	***0.44***	0.49	***0.69***	0.52	***0.69***	0.49	***0.69***
SCI	0.12	***0.22***	0.44	***0.56***	0.65	***0.89***	0.65	***0.89***	0.63	***0.83***
SW	0.40	***0.39***	0.44	***0.39***	0.64	***0.74***	0.64	***0.74***	0.50	***0.65***
SZ	0.33	***0.33***	0.42	***0.54***	0.58	***0.92***	0.61	***0.92***	0.44	***0.92***
XW	0.44	***0.47***	0.50	***0.60***	0.66	***0.93***	0.66	***1.00***	0.45	***0.80***
YJ	0.55	***0.56***	0.61	***0.56***	0.77	***0.94***	0.78	***0.94***	0.55	***0.88***
ZJ	0.60	***0.81***	0.57	***0.31***	0.71	***0.88***	0.72	***0.88***	0.48	***0.69***
ZH	0.38	***0.35***	0.54	***0.52***	0.66	***0.65***	0.67	***0.74***	0.39	***0.52***

Table 5. The same as Table 4, but for the comparisons of the average accuracy of the 3-day accumulated rainfall forecast.

City	The accuracy of EC		The 50% quantile scheme		The 100% quantile scheme with EC_{min}		The full quantile scheme with ECMWF extreme outputs		The 100% quantile scheme without ECMWF extreme output	
NA	0.00	***0.20***	0.20	***0.50***	0.26	***0.79***	0.27	***0.79***	0.25	***0.79***
SCI	0.03	***0.14***	0.31	***0.50***	0.46	***0.71***	0.46	***0.79***	0.43	***0.71***
SW	0.21	***0.44***	0.27	***0.44***	0.43	***0.72***	0.44	***0.72***	0.34	***0.67***
SZ	0.11	***0.37***	0.20	***0.37***	0.34	***0.79***	0.35	***0.79***	0.31	***0.68***

the extreme minimum still lacks practical significance for its harmlessness of the light rainfall. ECMWF model often underestimates the local rainfall of the whole area and the forecast by ECMWF model is usually too smooth to reflect the local rainstorm intensity which is more likely to lead to disastrous events. On the contrary, the coupled statistical scheme, which combines the outputs of ECMWF model and the historical observation information, can depict the rainfall well induced by TCs.

In forecasting the 3-day accumulated rainfall induced by TCs, the coupled statistical scheme also performs better than ECMWF model does. The rainfall forecast by the full quantile scheme with ECMWF extreme outputs and the 100% quantile scheme with EC_{min} overwhelm the ECMWF output at all the cities. The 50% quantile scheme and the 100% quantile scheme without ECMWF extreme output also outperform the ECMWF at 7 cities except for ZJ city.

It is worth noting that ECMWF model generally underestimates the extreme maximum rainfall and has a small forecasting range in forecasting the rainfall induced by TCs at a city area. Expanding the range appropriately can improve rainfall forecasting accuracy. However, there is a compromise between the forecasting rainfall range and the operational forecasting applicability. When the range is too large, such as the full quantile scheme with ECMWF extreme outputs, the applicability of the forecasting would be reduced though the accuracy is improved. And when the range is too small, such as the 50% quantile scheme, the forecast range might not include the extreme rainfall. Therefore, all the three coupled schemes should be referred to in the operational TC rainfall forecast.

3.3 *Case studies*

Besides the above general evaluations for ECMWF model and the coupled statistical boxplot schemes in forecasting TC induced rainfall, a particular TC case is employed in this study to assess the performance of these schemes. TC Kujira was a severe tropical storm that landed in 2015 (Fig. 3) and had a great impact in Guangdong province. The cities of SW, ZH, and YJ are used as the cities representing the east, middle and west parts of Guangdong province to illustrate the forecast performances of NWP model and the coupled statistical schemes.

In SW city, the maximum daily rainfall forecast by ECMWF model during the TC period is 24.58 mm, and the minimum daily rainfall is 1.97 mm (Fig. 4a). The forecasted rainfall range by ECMWF model cannot reflect the real situation of the rainfall observation ranging from 0 mm to 97mm (shown in Fig. 4c). On the contrary, the original boxplot scheme contains most of the range of the observed data (Fig. 4b). All the three coupled statistical schemes outperform the ECMWF model in forecasting the rainfall induced by TC Kujira at SW city. The 50% quantile scheme has an accuracy of 61%. The 100% quantile scheme with the EC_{min} and the full quantile scheme with ECMWF extreme outputs both have an accuracy of 93%, while ECMWF model only has an accuracy of 36%.

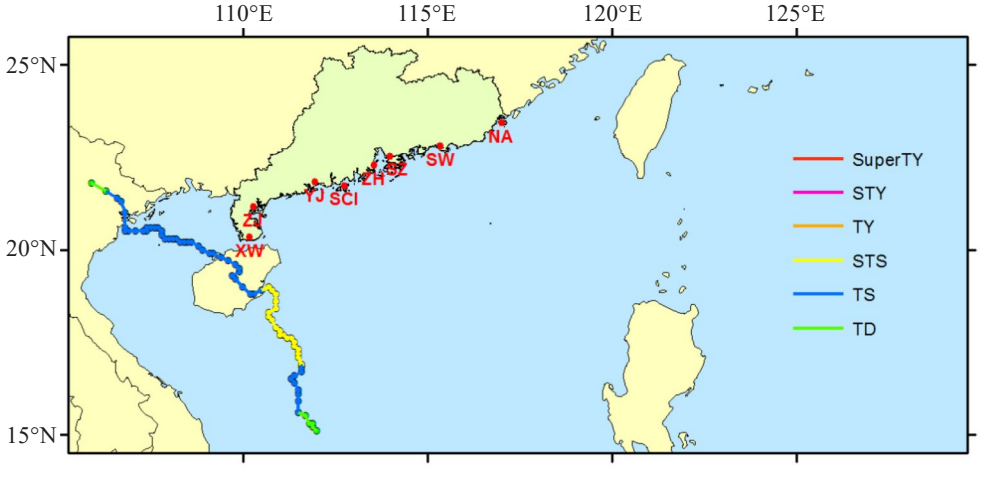

Figure 3. The track of TC Kujira (2015).

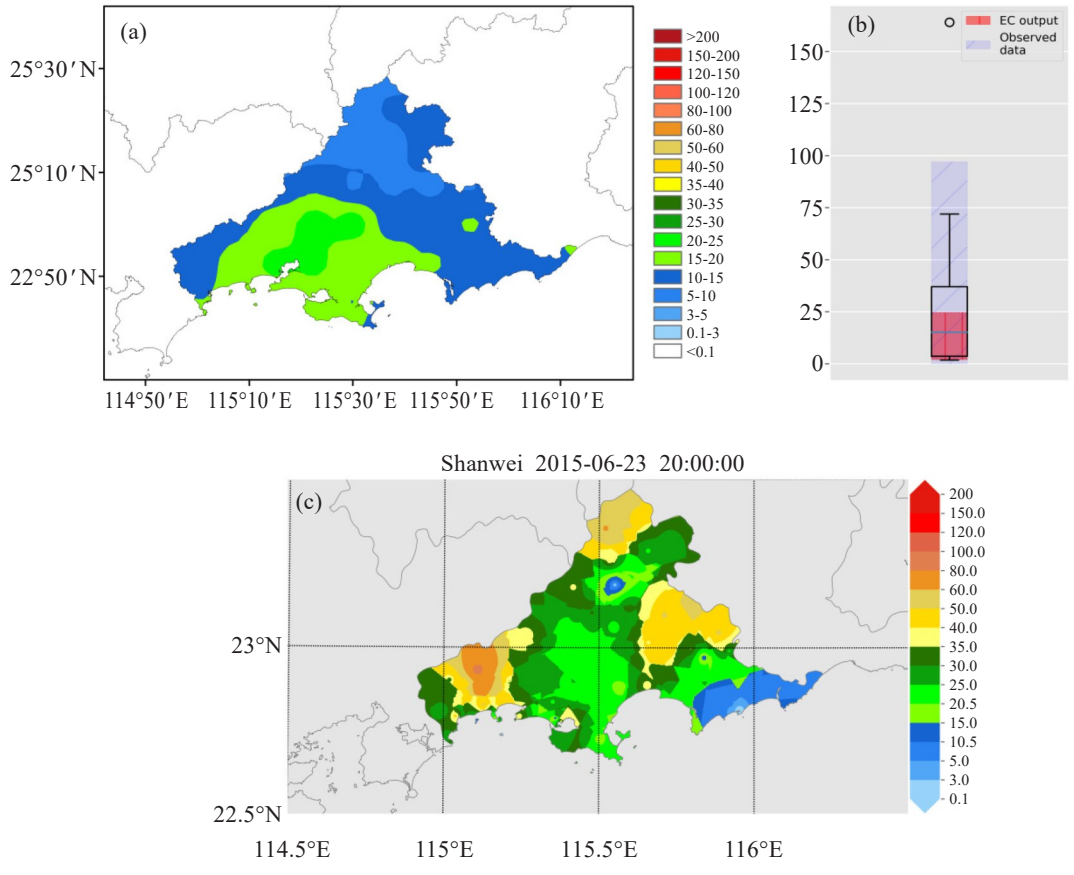

Figure 4. (a) The forecasted daily rainfall induced by TC Kujira at Shanwei by ECMWF model. (b) The boxplot of historical precipitation of the specific TC group. The red shadow represents the range of ECMWF output and the blue shadow represents the observed rainfall range. (c) The actual daily rainfall distribution in Shanwei.

In ZH and YJ, the situation is quite similar. In ZH, the maximum rainfall prediction by ECMWF model is 21mm and the minimum rainfall prediction is 7 mm, while the maximum observed rainfall is 45.5 and the minimum is 1. In YJ, the maximum rainfall prediction by ECMWF model is 30 and the minimum is 5; while the observed maximum rainfall is 84.5 and the minimum is 0. As Fig. 5 and Fig. 6 show, the ranges of the boxplots are larger than ECMWF model outputs, compared with the actual rainfall observation. The boxplots can therefore provide a good reference for weather forecasters. Actually in ZH, the 50% quantile scheme has an accuracy of 54%; the 100% quantile scheme with the EC_{min} and the full quantile scheme with ECMWF extreme outputs, both have an accuracy of 87.5%, while ECMWF model only has an accuracy of 33%. In YJ, the 50% quantile scheme has the accuracy of 44%; the 100% quantile scheme with EC_{min} and the full quantile scheme both have the accuracy of 84.4%, while ECMWF model has the accuracy of 31%.

From the above cases in the three cities, it can be inferred that ECMWF model has the shortage while forecasting the local rainfall induced by TCs and often underestimates the real rainfall range. Coupling ECMWF model forecast with the statistical boxplot could provide more accurate estimations of the local rainfall induced by TCs.

The situation is similar for the 3-day accumulated rainfall forecast along the coastal area. The ECMWF model forecasts are still too smooth to reflect the real situation and cannot predict the extreme situation. However, the statistical boxplot scheme and the coupled statistical schemes perform better. The comparisons are illustrated in Fig. 7, Fig. 8 and Fig. 9.

4 CONCLUSIONS

This study explores the methods to forecast the maximum daily rainfall and 3-day accumulated rainfall induced by landfalling TCs at the coastal cities in Guangdong province. The historical TCs landfalling in south China and in North Vietnam from 1951 to 2013 and the corresponding historical rainfall data at the coastal stations are used for the method calibration. The TCs and rainfall data from 2014 to 2017 are used for the method validation. Results show that the boxplot scheme based on the historical observation data can usually provide a better prediction of the rainfall range along the coastal city area than ECMWF model does. The performance of the coupled statistical boxplot schemes, with the integration of ECMWF model outputs into the

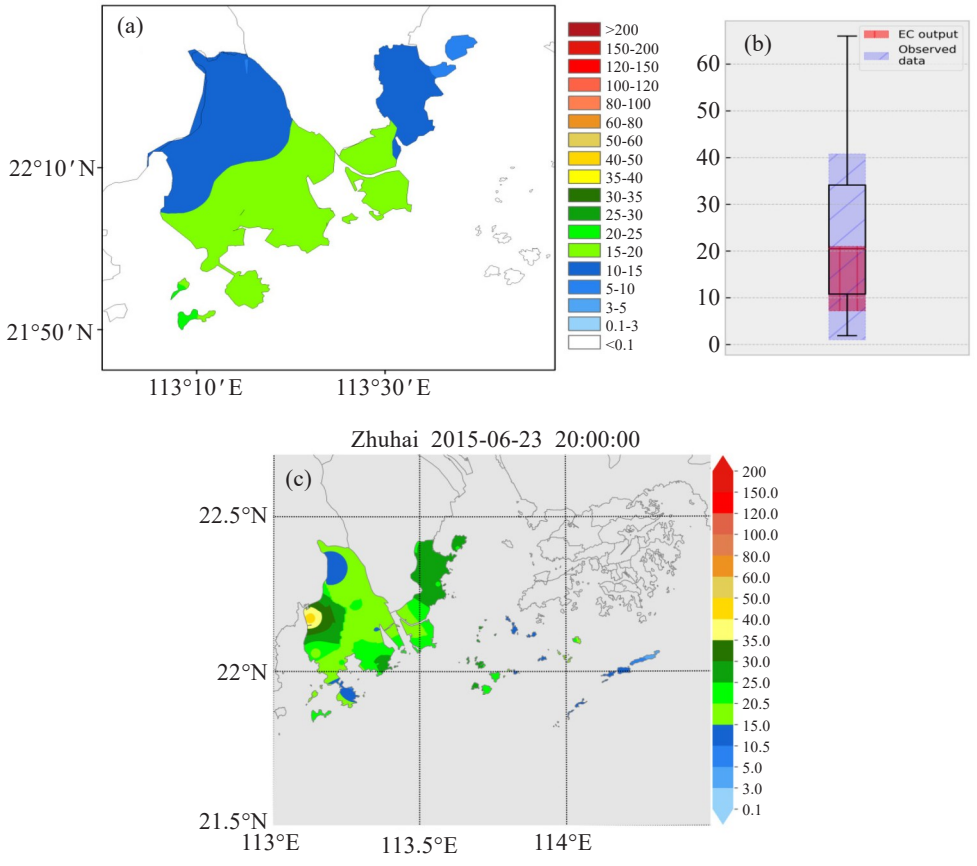

Figure 5. The same as Fig. 4, but for the city of Zhuhai.

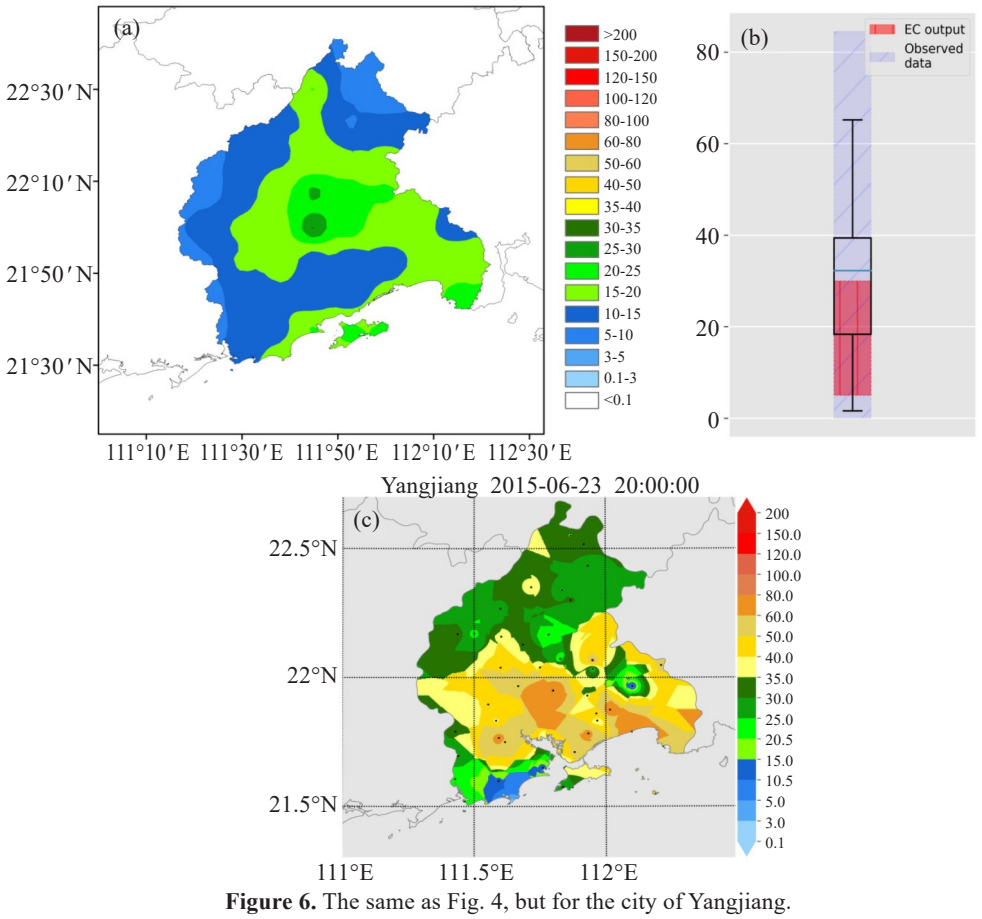

Figure 6. The same as Fig. 4, but for the city of Yangjiang.

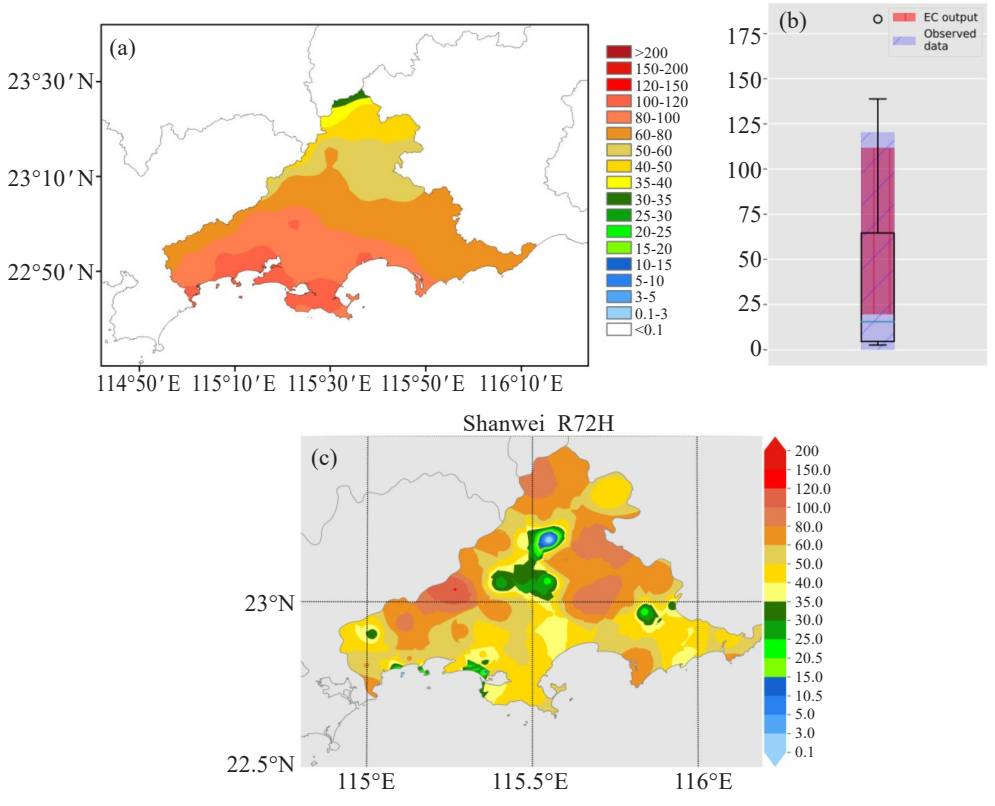

Figure 7. The same as Fig. 4, but for the 3-day accumulated rainfall in Shanwei.

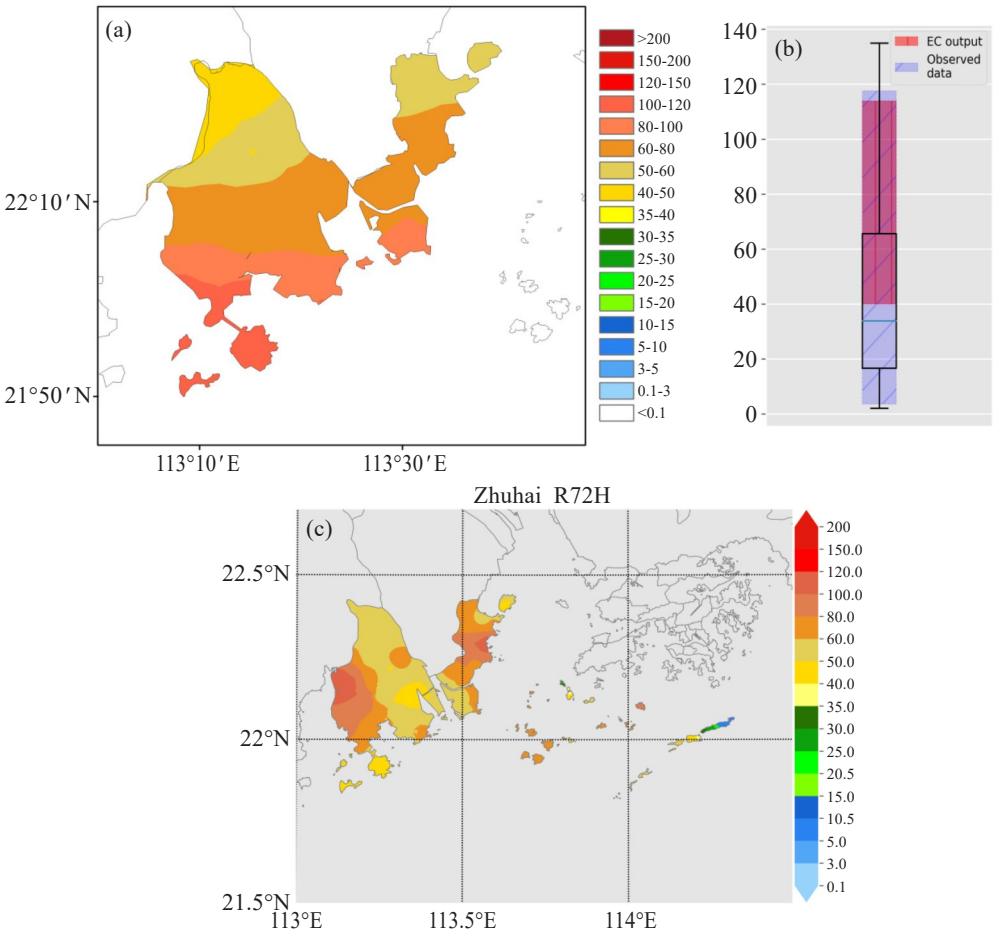

Figure 8. The same as Fig. 5, but for the 3-day accumulated rainfall in Zhuhai.

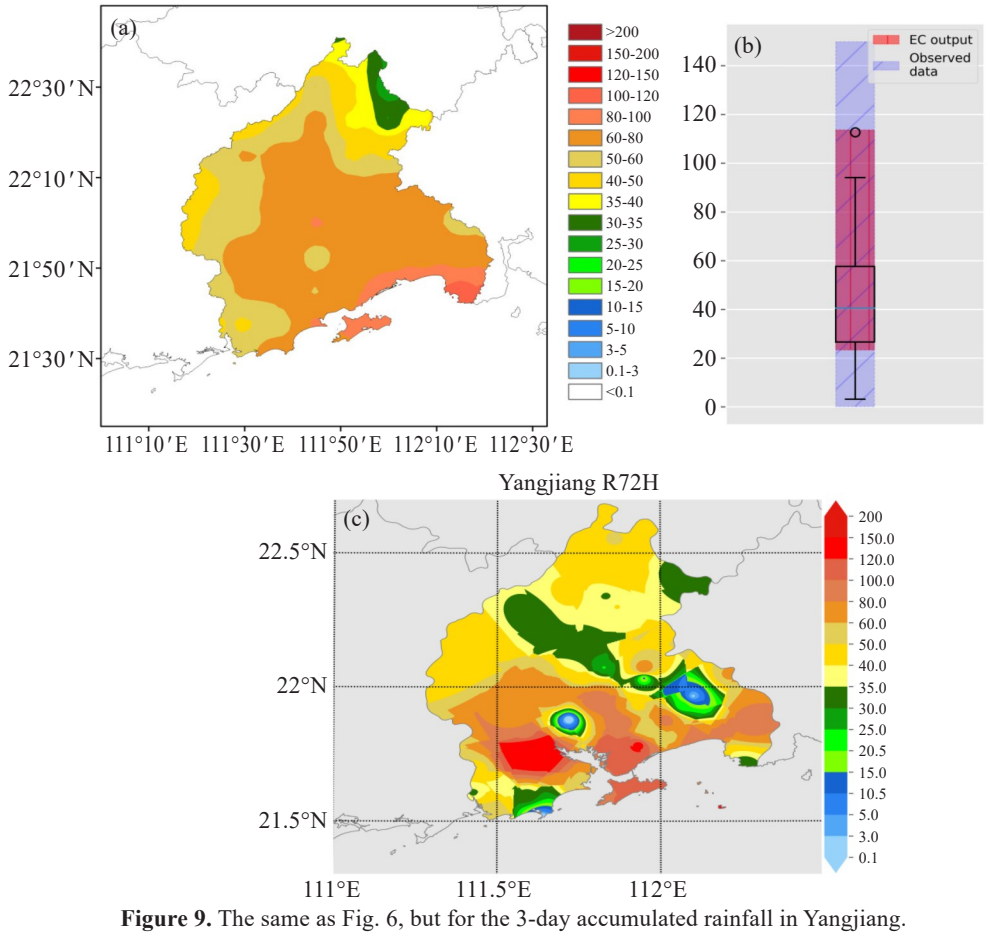

Figure 9. The same as Fig. 6, but for the 3-day accumulated rainfall in Yangjiang.

boxplot scheme, is further improved in forecasting the rainfall range at the coastal city area. The boxplot scheme and the coupled boxplot schemes are therefore valuable for forecaster in the real weather forecast operation during TC seasons.

REFERENCES:

[1] REN F M, GLEASON B, EASTERLING D. Typhoon impacts on China's precipitation during 1957-1996 [J]. Adv Atmos Sci, 2002, 19(5): 943-952, https://doi. org / 10.1007/s00376-002-0057-1.

[2] XIAO F J, XIAO Z N. Characteristics of tropical cyclones in China and their impacts analysis [J]. Natural Hazards, 2010, 54(3): 27-837, https://doi.org / 10.1007 / s11069-010-9508-7.

[3] RAPPAPORT E N, FUCHS M, LORENSTON M. The threat to life in inland areas of the United States from Atlantic tropical cyclones [C]// 23d Conference on Hurricanes and Tropical Meteorology, Dallas: American Meteorological Society, 1999, 811-814.

[4] LI Q L, XU P C, WANG X B, et al. An operational statistical scheme for tropical cyclone induced wind gust forecast [J]. Wea Forecasting, 2016, 31(6): 1817-1832, https://doi.org/10.1175/waf-d-16-0015.1.

[5] BUSINGER S, KNAPP D I, WATSON G F. Storm following climatology of precipitation associated with winter cyclones originating over the Gulf of Mexico [J]. Wea Forecasting, 1990, 5(3): 378-403, https://doi. org / 10.1175/1520-0434(1990)005<0378:sfcopa>2.0.co;2.

[6] AMS. Policy statement: Hurricane research and forecasting [J]. Bull Amer Meteor Soc, 2000, 81(6): 1341-1346, https://doi.org/10.1175/1520-0477(2000)081<1341:pshraf>2.3.co;2.

[7] WILLOUGHBY H E, RAPPAPORT E N, MARKS F D. Hurricane forecasting: The state of the art [J]. Natural Hazards Review, 2007, 8(3): 45-49, https://doi.org/10.1061/(ASCE)1527-6988(2007)8:3(45).

[8] ROY C, KOVORDANYI R. Tropical cyclone track forecasting techniques-A review [J]. Atmos Res, 2012, 104-105: 40-69, https://doi.org/10.1016/j.atmosres.2011.09.012.

[9] SAHA K K, HASAN M M, QUAZI A. Forecasting tropical cyclone-induced rainfall in coastal Australia: implications for effective flood management [J]. Australasian J Environ Management, 2015, 22(4): 446-457, https://doi. org / 10.1080/14486563.2015.1028109.

[10] LONFAT M, MARKS Jr. F D, CHEN S S. Precipitation distribution in tropical cyclones using the Tropical Rainfall Measuring Mission (TRMM) microwave imager: A global perspective [J]. Mon Wea Rev, 2004, 132(7): 1645-1660, https://doi.org/10.1175/1520-0493(2004)132<1645:pditcu>2.0.co;2.

[11] RIEHL H, MALKUS J. Some aspects of Hurricane Daisy [J]. Tellus, 1961, 13(2): 181-213, https://doi.org/10.1111/j.2153-3490.1961.tb00077.x.

[12] SIMPSON R H, RIEHL H. The Hurricane and Its Impact [M]. Louisiana State University Press, 1981: 135-140.

[13] KIDDER S Q, KNAFF J A, KUSSELSON S J, et al. The

tropical rainfall potential (TRaP) technique, Part I: Description and examples [J]. Wea Forecasting, 2005, 20 (4): 456-464, https://doi.org/10.1175/waf860.1.

[14] PFOST R L. Operational tropical cyclone quantitative precipitation forecasting [J]. National Weather Digest, 2000, 24(1-2): 61-66.

[15] ELSBERRY R L. Predicting hurricane landfall precipitation: Optimistic and pessimistic views from the symposium on precipitation extremes [J]. Bull Amer Meteor Soc, 2002, 83(9): 1333-1339, https://doi. org / 10.1175/1520-0477(2002)083<1333:phlpoa>2.3.co;2.

[16] CORBOSIERO K L, MOLINARI J. The relationship between storm motion, vertical wind shear, and convective asymmetries in tropical cyclones [J]. J Atmos Sci, 2003, 60(2): 366-376, https://doi.org/10.1175/1520-0469(2003)060<0366:trbsmv>2.0.co;2.

[17] KIMBALL S K. Structure and evolution of rainfall in numerically simulated landfalling hurricanes [J]. Mon Wea Rev, 2008, 136(10): 3822-3847, https://doi. org / 10.1175/2008mwr2304.1.

[18] LI Q L, LAN H P, CHAN J C, et al. An operational statistical scheme for tropical cyclone induced rainfall forecast [J]. J Trop Meteor, 2015, 21(2): 101-110, https://doi.org/10.16555/j.1006-8775.2015.02.001.

[19] MARKS F D, KAPPLER G, DEMARIA M. Development of a tropical cyclone rainfall climatology and persistence (R-CLIPER) model [C]// 25th Conference on Hurricanes and Tropical Meteorology, San Diego: American Meteorological Society, 2002.

[20] LONFAT M, ROGERS R, MARCHOK, T, et al. A parametric model for predicting hurricane rainfall [J]. Mon Wea Rev, 2007, 135(9): 3086-3097, https://doi.org/10.1175/mwr3433.1.

[21] LIANG B Q, LIANG J Q, WEN Z P. The characteristics of typhoon disasters and its effects on economic development in Guangdong province [J]. Natural Disaster Reduction in China, 1994, 49(4): 145-150 (in Chinese).

[22] YE W. The Characteristics of typhoon disaster and disaster countermeasures in Guangdong Province [J]. Journal of Catastrophology, 2002, 17(3): 54-59 (in Chinese).

[23] YUAN J N, ZHENG B. An analysis on interdecadal variations of tropical cyclone precipitation in Guangdong province of China [J]. J Trop Meteor, 2012, 18(1): 65-71, https://doi.org/10.3969/j.issn.1006-8775.2012.01.007.

[24] YIN J, WU S, DAI E. Assessment of economic damage risks from typhoon disasters in Guangdong, China [J]. J Resources and Ecology, 2012, 3(2): 144-150, https://doi.org/10.5814/j.issn.1674-764x.2012.02.006.

[25] XINHUANET NEWS. Typhoon Mujigae kills 19 in south China, 06 Oct 2015. Accessed September 22, 2017 [Available Online at: http://news.xinhuanet.com/english/2015-10/06/c_134687953.htm]

[26] CHEN L S, LI Y, CHENG Z Q. An overview of research and forecasting on rainfall associated with landfalling tropical cyclones [J]. Adv Atmos Sci, 2010, 27(5): 967-976, https://doi.org/10.1007%2Fs00376-010-8171-y.

[27] XU Y L, ZHANG L, GAO S Z. The advances and discussions on China operational typhoon forecasting [J]. Meteorol Mon, 2010, 36(7): 43-49, https://doi. org / 10.3788/HPLPB20102207.1462.

[28] PETT M A. Nonparametric Statistics for Health Care Research-Statistics for Small Samples and Unusual Distributions [M]. Thousand Oaks: Sage Publications, 1997: 307.

[29] WILKS D S. Statistical Methods in the Atmospheric Sciences (Vol. 100) [M]. Academic Press, 2011: 23-24.

[30] TUKEY J W. Exploratory Data Analysis [M]. Menlo Park, Cal, London, Amsterdam, Don Mills, Ontario: Addison-Wesley Publishing Company Reading, Mass, 1977: 688.

[31] JOHNSON G L, DALY C, TAYLOR G H, et al. Spatial variability and interpolation of stochastic weather simulation model parameters [J]. J Applied Meteorol, 2000, 39(6): 778-796, https://doi.org/10.1175/1520-0450(2000)039<0778:SVAIOS>2.0.CO;2.

[32] CHOWDHURY A F M K, LOCKART N, WILLGOOSE G, et al. Development and evaluation of a stochastic daily rainfall model with long-term variability [J]. Hydrology and Earth System Sciences, 2017, 21(12): 6541-6558, https://doi.org/10.5194/hess-21-6541-2017.

[33] ONYUTHA C, WILLEMS P. Space-time variability of extreme rainfall in the River Nile basin [J]. International Journal of Climatology, 2017, 37(14): 4915-4924, https://doi.org/10.1002/joc.5132.

[34] HALPERIN D J, FUELBERG H E, HART R E, et al. An evaluation of tropical cyclone genesis forecasts from global numerical models [J]. Wea Forecasting, 2013, 28 (6): 1423-1445, https://doi. org / 10.1175 / WAF-D-13-00008.1.

[35] WANG Y, BELLUS M, GELEYN J F, et al. A new method for generating initial condition perturbations in a regional ensemble prediction system: Blending [J]. Mon Wea Rev, 2014, 142(5): 2043-2059, https://doi. org / 10.1175/MWR-D-12-00354.1.

[36] MAGNUSSON L, BIDLOT J R, LANG S, et al. Evaluation of medium-range forecasts for hurricane Sandy [J]. Mon Wea Rev, 2014, 142(5): 1962-1981, https://doi.org/10.1175/MWR-D-13-00228.1.

[37] ZHONG Shui-xin, YANG Shuai and CHEN Zi-tong. Evaluation of the parameterization schemes and nudging techniques in GRAPES for warm sector torrential rains using surface observations [J]. J Trop Meteor, 2019, 25(3): 353-364, https://doi.org/10.16555/j.1006-8775.2019.03.007.

[38] YATES E, ANQUETIN S, DUCROCQ V, et al. Point and areal validation of forecast precipitation fields [J]. Meteorol Appl, 2006, 13(1): 1-20, https://doi.org/10.1017/S1350482705001921.

Citation: LI Qing-lan, LIU Bing-rong, WAN Qi-lin, et al. Operational forecast of rainfall induced by landfalling tropical cyclones along Guangdong coast [J]. J Trop Meteor, 2020, 26(1): 1-13, https://doi.org/10.16555/j.1006-8775.2020.001.